Turk J Chem
26 (2002) , 759 – 769.


# Corrosion of Reinforcing Steel in Concrete Immersed in Chloride Solution and the Effects of Detergent Additions on Diffusion and Concrete Porosity

**Hülya KAHYAOĞLU**
*Niğde University, Faculty of Education*
*51100 Niğde-TURKEY*
**Mehmet ERBİL, Birgül YAZICI**
*Çukurova University, Faculty of Science and Art, Department of Chemistry,*
*01330 Adana-TURKEY*
**Ayse Bahar YILMAZ***
*Mustafa Kemal University, Faculty of Fisheries,*
*31040 Antakya-TURKEY*
*e-mail: aybahar@yahoo.com*

Received 06.11.2001

In order to investigate the corrosion of reinforcing steel in concrete and the effects of chloride ions, oxygen diffusion and detergent additives of linear alkylbenzene (LAB) and linear alkylbenzene sulfonate (LAS), potentiokinetic experiments were carried out. Thus, by embedding steel electrodes into concrete specimens with a water/cement (W/C) ratio of 0.45, current-potential curves were obtained and the compressive strength of the specimens was measured. The electrochemical approach can be used to identify the effect of chloride on steel corrosion in concrete. It was found that the diffusion of chloride and oxygen through concrete and the reduction of oxygen on the metal surface are important parameters controlling reinforcing steel corrosion.

## Introduction

Reinforced concrete is one of the most common construction materials. High-quality reinforced concrete is obtained under the following conditions: correct cure times, correct positioning of the steel reinforcement, an appropriate water/cement ratio and the correct use of aggregate. If these conditions are met then corrosion of the reinforcing steel is generally negligible because the high pH in concrete renders the steel passive[1−4]. As the diffusion rate of oxygen and water from the atmosphere is low, the passive film is relatively stable and reinforcing steel does not generally corrode[5,6]. However, there are two main mechanisms causing corrosion of reinforcing steel. Firstly, $CO_2$ from the atmosphere diffuses into the concrete and lowers the pH. If the pH falls sufficiently, the steel may no longer be passive and general corrosion starts. Secondly, chloride ions, either present initially or by diffusion from the external environment, can initiate pitting corrosion.

*Corresponding author

Generally, metal corrosion cannot be prevented in environments containing active ions like chloride[7,8]. When present initially, chloride can prevent or slow the formation of a passive film, or the re-passivation reaction. When present at a pre-existing passive film, breakdown of the film may occur at flaws. Both processes result in pitting corrosion.

In concrete, chloride may arise from the initial mixing water. Alternatively, external sources can penetrate into the concrete from microcracks or capillary pores at a later stage. The factors that affect the depth of penetration are commonly as follows: chloride concentration of the external solution, the time of contact with the salt solution, the cation present and the concrete quality (ratio of water/cement, the time of curing and curing conditions, temperature etc.)[9−12]. If in the preserve of chloride ions, the passive film on the metal surface undergoes disruption that may result eventually in pitting of the rebar[1]. In addition, corrosion products cause an expansion in volume and thus can lead to internal stresses and even to macroscopic cracking of the concrete[13]. As a result, the strength of the reinforced concrete is reduced. Finally, as a result of the reaction of chloride ions with certain cements, re-crystallization can occur primarily in high aluminum containing mixtures forming calcium chloro-aluminates ($3CaO.Al_2O_3.CaCl_2.10H_20$)[14], which have poor strength.

The effects of waste pollutants on concrete and reinforcing steel should also be taken into account together with some ions found in mixing water. For example, one of these wastes is linear alkylbenzene sulfonate (LAS), which is one of the main compounds in synthetic detergents is and produced by the sulfonation of linear alkylbenzene (LAB). LAB and LAS are found together in water because of part sulfonation of LAB and run to waste. Thus, concrete mixing waters may contain LAS and LAB in addition to $Cl^-$ and $SO_4^=$ ions. LAS and LAB may also be added deliberately. As detergents, they lower water surface tension and can help to improve concrete wet mixability and reduce set concrete porosity.

Therefore, in the present study, reinforced concrete specimens were prepared using various mixing waters containing variously distilled water, and NaCl with additions of LAS and LAB. The corrosion of reinforcing steel and concrete strength of these specimens were investigated after curing in 1 M NaCl external solution.

# Experimental Details

## Materials

The cement used was composed of 28.99% $SiO_2$, 7.08% $Al_2O_3$, 2.82% $Fe_2O_3$, 0.42% $Mn_2O_3$, 51.17% CaO, 3.17% MgO, 2.26 $SO_3$, 1.02 $K_2O$ and 0.67% free CaO. Natural aggregate was used in the experiments. The dry surface density of the aggregate was 2.63 x $10^3$ kg $m^{-3}$ and the size ranges were 0.5-4 mm and 4-8 mm. The mixing water compositions are shown in Table 1 (the purity of LAS and LAB was 96.5%). The water/cement ratio (W/C) of the specimens was 0.45, and the steel composition was 0.13% C, 0.65% Mn, 0.030% S, 0.013 %P and 0.017% Si. The final composition of the concrete is given in Table 2.

## Test specimens and conditioning

The concrete specimens were removed from the mould 24 h after placement and post-cured for 24 h in 1 M NaCl, after which the experiments were started. The three electrode (potentiodynamic) technique was used in electrochemical measurements. The reference electrode was a saturated calomel electrode (SCE) and Pt

($10^{-4}$ $m^2$) was used as a counter electrode, both in the external 1 M NaCl electrolyte. The measurements were carried out on days 1, 2, 7, 28 and 60 of curing. Current and voltage values were read potentiokinetically with a potentiostat having a scan rate of $10^{-4}$ V $s^{-1}$. The tests were made in conditions open to the atmosphere and the solutions were stirred with a magnetic stirrer during measurements. Each potential scan took about 3 h.

**Table 1.** The compositions of mixing water and external solution, and the measured compressive strength of the concrete specimens after 28 days of curing

| Working environments | External solution | Mixing water | 28 day compressive strength /MPa |
|---|---|---|---|
| 1 | 1 M NaCl | Distilled water | 31.03 |
| 2 | 1 M NaCl | Distilled water + 300 ppmLAS | 45.62 |
| 3 | 1 M NaCl | Distilled water + 300 ppmLAB | 47.15 |
| 4 | 1 M NaCl | 1 M NaCl | 34.25 |
| 5 | 1 M NaCl | 1 M NaCl + 300 ppm LAS | 39.63 |
| 6 | 1 M NaCl | 1 M NaCl + 300 ppm LAB | 41.81 |

**Table 2.** Composition of the concrete

| | Mass / kg | Density /kg $dm^{-3}$ | Volume /$dm^3$ |
|---|---|---|---|
| Water | 191 | 1.00 | 191 |
| Cement | 424.44 | 2.96 | 143.4 |
| Agregate | 1697.9 | 2.63 | 645.6 |
| Air | - | - | 20 |

Current-potential and compressive strength measurements were repeated three times at each time and reproducible results were obtained and are presented here.

In the mechanical experiments, cubic concrete specimens (0.15 x 0.15 x 0.15m) were used. The compressive strengths of these specimens, in MPa, were measured after curing for 28 d in external solution (1 M NaCl) using a Tonitecnic[15].

## Results

## Current-potential curves

The current-potential curves are plotted with the values measured on days 1 and 60; data obtained between these times were not sufficiently distinguishable. In Figure 1, the current-potential curves of the specimens prepared with distilled water and cured in 1 M NaCl external solution are shown. The current gradually decreased when polarized from –1.8 V in the anodic direction. The system reached a mixed potential (i.e. the current became zero) at about -1.0 V on the first day of curing (Fig. 1a) and about -0.8V on day $60^{th}$ (Fig. 1b). In Figure 1a, in the anodic potential region there are two step-like current changes at potentials of -0.8 V and -0.5 V but the current starts to increase again at 0.0 V.

The current-potential relationship shows a similar pattern for days 1 and 60, as seen in Figures 1a and 1b. However, the potentials at which the current increases shift to the more positive potential region in Figure 1b. All of these current changes take place until +1.8V is reached. On the reverse sweep, the current continues to decrease until the mixed potential, which has shifted to about -0.2 V on day 60 (Fig.

1b) compared with about -0.5 V on the first day (Fig. 1a). The curves are similar in Figures 1a and 1b, except for the change in the mixed potential values. Lower current values were measured at all potentials on day 60 (Fig. 1b) compared to the first day (Fig. 1a).

In Figure 2, the current-potential curves of the specimens prepared with mixing water (distilled water + 300 ppm LAS) and cured in 1 M NaCl external solution are shown. When the system was polarized with an initial potential of -1.8 V, in the anodic direction, the mixed potential was -1.0 V on day 1 (Fig. 2a) and -0.8 V on day 60 (Fig. 2b). The current increase slows at about -0.5 V and then at about 0.0 V the current increase starts again. In the case of cathodic polarization, with an initial potential of +1.8 V, the curve continues to decrease until -0.6 V on day 1 and until -0.5 V on day 60. After the mixed potential the curve pattern is similar to that in anodic polarization. On day 60, the current values were lower than those on day 1 at the same potentials (Figs. 2a and 2b).

In Figure 3, the current-potential curves of the specimens prepared with mixing water (distilled water + 300 ppm LAB) and cured in 1M NaCl external solution are shown. As seen in Figures 3a and 3b, when the system was polarized in the anodic direction from the initial potential of -1.8 V, the system reached about the same mixed potential value of -1.0 V on days 1 and 60 and the current with it became zero. On day 1, the current increased to -0.5 V, except for a small decrease in current around -0.9 V. There was a decrease in current between -0.5 V and 0.0 V. Then the current started to increase after 0.0 V. On day 60, there was a continuous change in current with it increasing between -1.0 V and +1.8 V. The system again reached about the same mixed potential value of -0.5 V when polarized in the cathodic direction on both days 1 and 60 and the current-potential curves became similar in shape, as shown in Figures 3a and 3b.

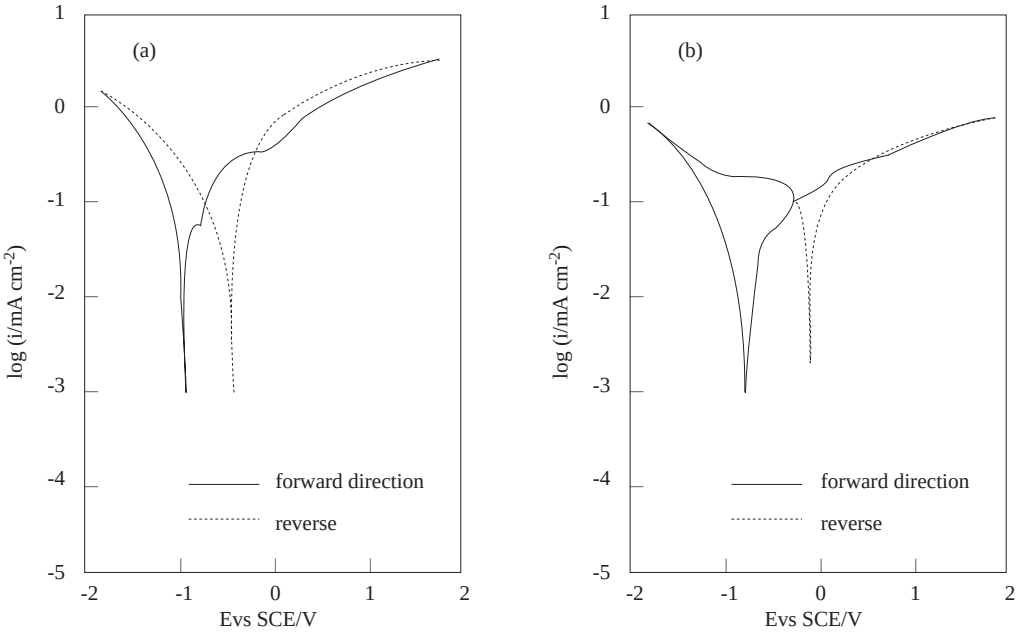


**Figure 1.** Semilogarithmic current-potential curves, system: Fe/1 M NaCl; Mixing water: Distilled water (a:day 1, b:day 60)

In Figures 4, 5 and 6, the current potential curves obtained in the same external solutions as before of the specimens prepared with the solutions of 1 M NaCl (Fig. 4), 1 M NaCl + 300 ppm LAS (Fig. 5) and 1 M NaCl + 300 ppm LAB (Fig. 6) as mixing waters are shown. The curves are very similar in shape for

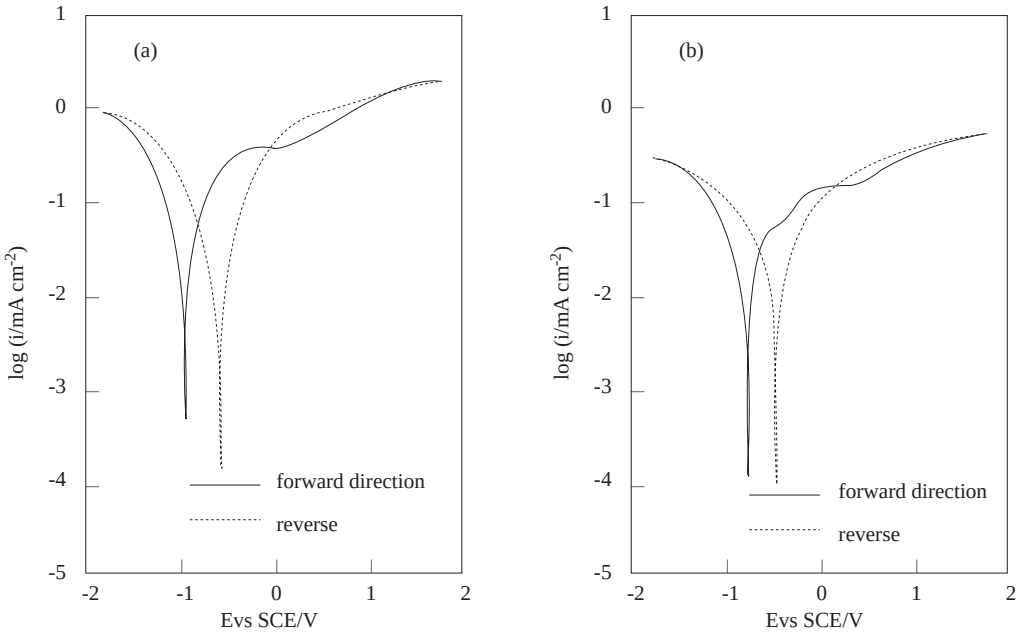


**Figure 2.** Semilogarithmic current-potential curves, system: Fe/1 M NaCl; Mixing water: Distilled water + 300 ppm LAS (a:day 1, b:day 60)

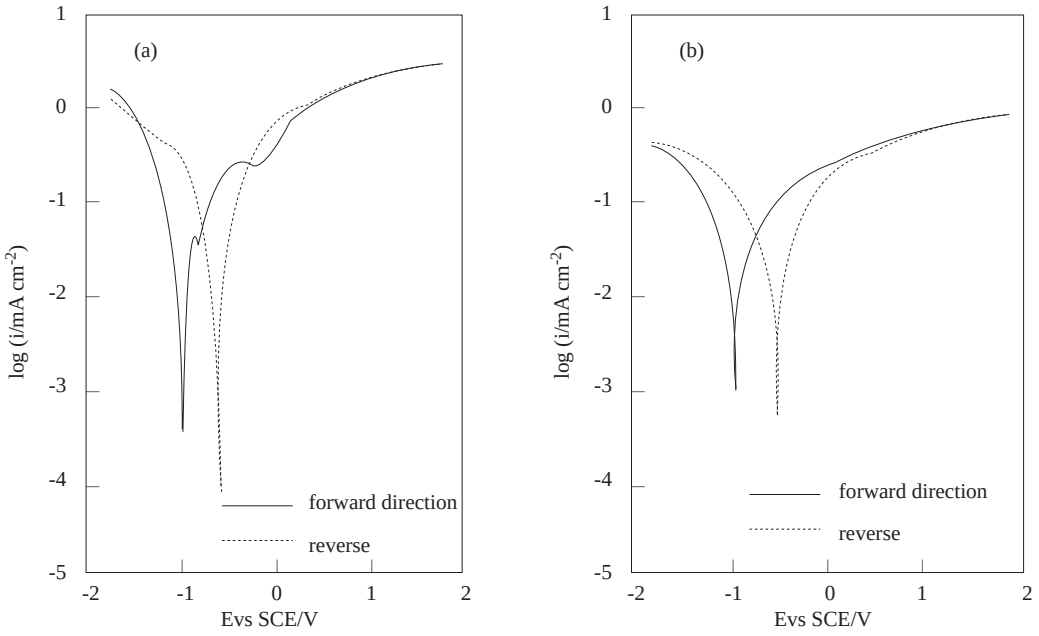


**Figure 3.** Semilogarithmic current-potential curves, system: Fe/1 M NaCl; Mixing water: Distilled water + 300 ppm LAB (a:day 1, b:day 60)

all of the specimens. On day 1, when the systems were polarized in the anodic direction with an initial potential of -1.8 V, they reached a mixed potential around -1.0 V. There was a current increase up to -0.5 V and a decrease in current between -0.5 V and 0.0 V for all cases as shown in Figures 4, 5 and 6. After 0.0 V, the current continued to increase until +1.8 V; but as seen in Figures 5a and 6a, there a slight temporary

decrease in current around -0.9 V. When the systems were polarized in cathodic direction starting from +1.8 V, identical curve shapes were obtained and the mixed potential was 0.5 V for all cases. Current values were lower on day 60 compared to those on day 1.

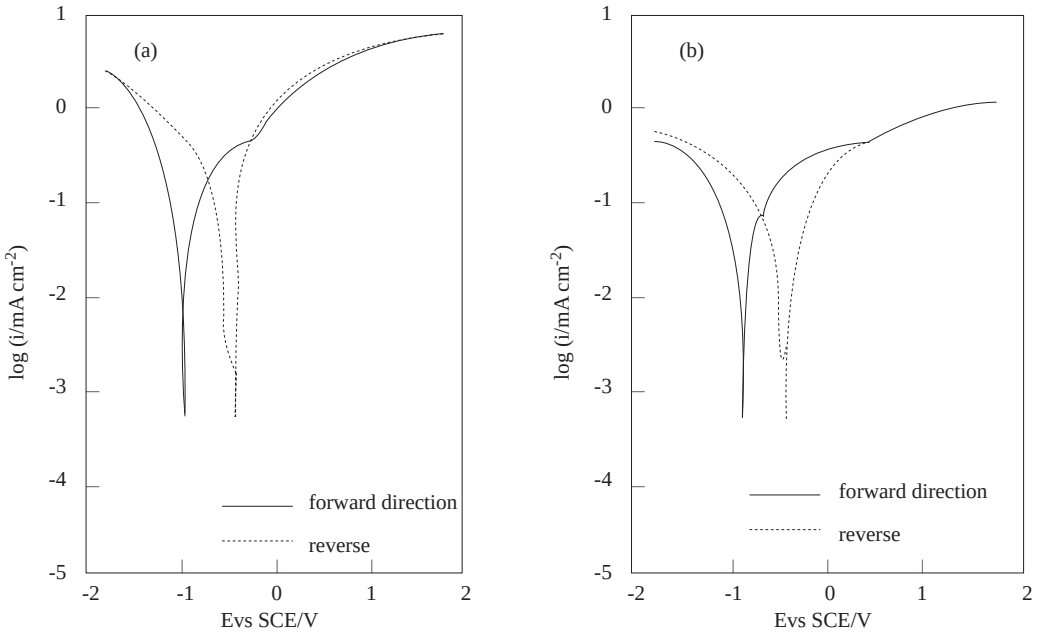


**Figure 4.** Semilogarithmic current-potential curves, system: Fe/1 M NaCl; Mixing water: 1 M NaCl (a:day 1, b:day 60)

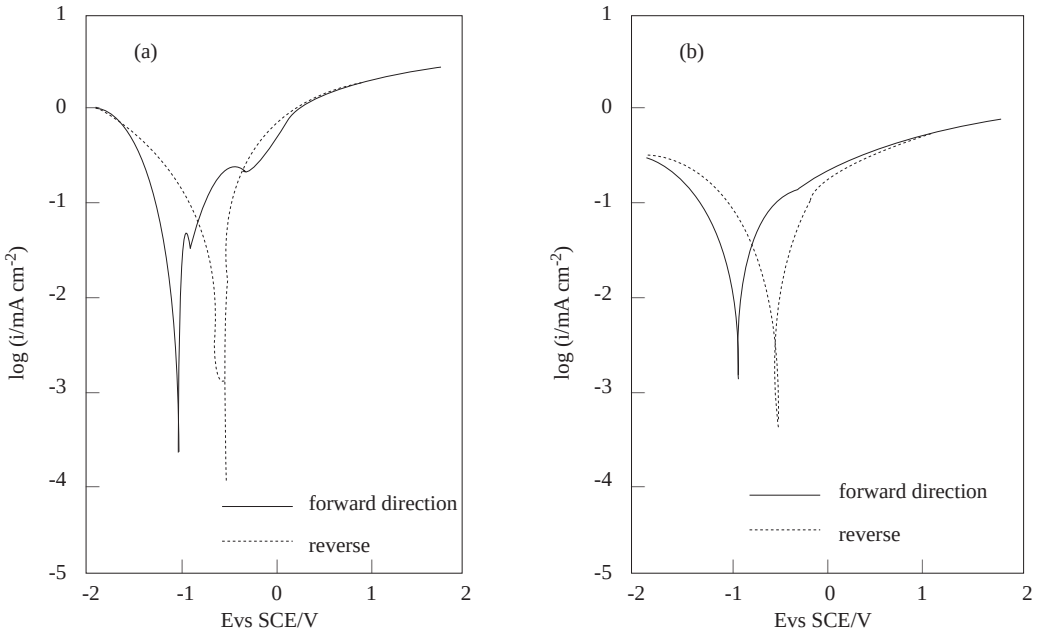


**Figure 5.** Semilogarithmic current-potential curves, system: Fe/1 M NaCl; Mixing water: 1 M NaCl + 300 ppm LAS (a:day 1, b:day 60)

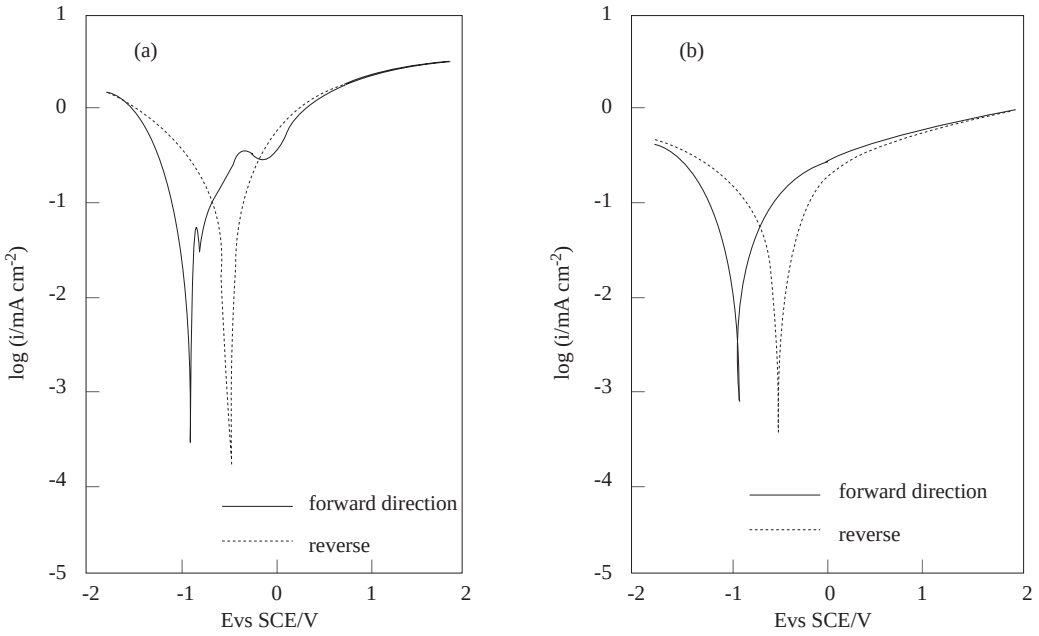


**Figure 6.** Semilogarithmic current-potential curves, system: Fe/1 M NaCl; Mixing water: 1 M NaCl + 300 ppm LAB (a:day 1, b:day 60)

### Compressive strength

In Table 1, the compressive strength values of specimens cured for 28 days are given. The compressive strength values of the specimens for environments 1, 2 and 3 were 31.03 MPa, 45.62 MPa and 47.15 MPa respectively. For environments 4, 5, and 6, the strength values were 34.25 MPa, 39.63 MPa and 41.81 MPa respectively.

## Discussion

Concrete is a construction material with a high compressive strength. Embedding steel rods into the concrete structure gives an increase in strength due to the stiffness provided by the rods. The compressive strength of concrete also depends on the composition and the size of aggregate, water/cement ratio etc.

The major parameters controlling the corrosion of reinforcing steel may be given as follows[13,16,17]:

1- Carbonation of the concrete, which lowers its pH.

2- Chloride and sulfate ions in concrete.

3- The porosity of concrete controlling diffusion of ions in water and, importantly, oxygen.

The high pH values of concrete cause surface passivation in reinforcing steel[15]. Therefore any free chloride ions existing in the concrete, are expected to initiate pitting corrosion[18−20]. To prevent this, the amount of initial free $Cl^-$in concrete must be low or the diffusion of chloride ions into the concrete structure must be prevented[2,19]. It is reported that chloride ions can cause an increase in the local corrosion rate by about $10^2$-$10^3$ times[21−23]. However, under our experimental conditions the change in current indicates an increase of 2-3 times with $Cl^-$ compared to $Cl^-$ free mixing water. This is because the total current measured here does not reflect fully any local pitting. It is still, nevertheless, a good guide of corrosion onset. In concrete, not all $Cl^-$ is free to diffuse and some may be lowered by the reaction in the cement paste.

Nevertheless, the diffusion of chloride ions depends on concrete porosity[10]. An additional factor affecting the corrosion rate is oxygen in the concrete[3,6,20]. Therefore low porosity is also good for preventing the diffusion of oxygen into the concrete from the environment. The oxygen diffusion rate depends on the fraction of water filled pores to open pores. If the pores are open, then the diffusing rate can be light, while water-filled pores can slow oxygen diffusion. The diffusion of oxygen can be equal to the resistance to diffusion (concrete resistance) $R_c$. The oxygen reduction rate on the metal surface depends on the polarization resistance ($R_p$). The total resistance for oxygen reduction can be given as the sum of these resistances:

$$R_t = R_c + R_p \tag{1}$$

The oxygen diffusion coefficient ($Do_2$) for water is given as $2.1.10^{-9}$ $m^2$ $s^{-1}$ at 20°C[24], and the oxygen solubility in 1 M NaCl external solution is ~ 6.8 ppm (20°C)[24]. Considering the above given oxygen solubility and imagining that concrete acts like water, then according to Fick's First Law:

$$J(eq.m^{-2}s^{-1}) = -D\frac{dc}{dx} \tag{2}$$

the amount of oxygen (J) diffused through the concrete per square meter per second can be calculated for the conditions given above as follows:

dC ≅ $C_0$ = 6.8 ppm (C = 0, at limiting current)

dx = $10^{-2}$ m (concrete thickness of working electrode)

J = $-2.1.10^{-9}$ $m^2s^{-1}.6.8$ $g.ton^{-1}(m^3)^{-1}.1$ eq.8 $g^{-1}.10^2$ $m^{-1}$ = $-1.785.10^{-7}$ eq. $m^{-2}$ $s^{-1}$

Thus, the expected limiting current ($i_L$) should be $i_L = 1.72.10^{-2}$ A $m^{-2}$ in order to reduce this amount of oxygen ($i_L = 1.785.10^{-7}$ x 96500 = $1.72.10^{-2}$ A $m^{-2}$). In these experiments such a low limiting current value was not observed (Figs. 1-6). However, concrete should not be expected to behave like water. In previous studies, the limiting current for oxygen diffusion in concrete was given as $i_L = 5.10^{-4}$ A $m^{-2}$ [6] and depended on the concrete composition. In this study, no limiting current was obtained and all the measured current values were higher than these values (Figs. 1-6). Using the above values,

J = $1.785.10^{-7}$eq. $m^{-2}$ $s^{-1}$

$i_L = 1.72.10^{-2}$ A $m^{-2}$ (calculated cathodic oxygen reduced limiting current in water)

$i_L = 5.10^{-4}$A $m^{-2}$ {measured limiting current by[6]}

a new oxygen diffusion coefficient for concrete can be determined as

$Do_2 = 6.1.10^{-11}$ $m^2$ $s^{-1}$

The water/cement ratios of the electrodes used in the experiments were slightly different from those in the literature[6]. However, the result helps to give an approximate value for the diffusion coefficient. Further, the value is in agreement with those in the literature[5,6,25].

The pH dependence of oxygen and hydrogen reduction, which are the two basic cathodic reactions, are given by the following equations:

$$O_2/OH^-, E = 1.227 - 0.059pH(SHE) \tag{3}$$

$$H^+/H_2, E = -0.059pH(SHE) \tag{4}$$

According to these, oxygen reduction should be expected at potentials below 0.328 V (SCE) at average measured concrete pH values of 11 in the experimental conditions open to the atmosphere. Hydrogen reduction should be expected at potentials below -0.900 V (SCE). Although hydrogen reduction is not important for rebar corrosion normally as the mixed potential is much more positive than –900 mV (SCE), it is of interest in the cathodic protection of rebar and also at the cathodic potentials used in this experiment. Normally hydrogen evolution must be avoided as it breaks the steel/concrete bond and causes hydrogen embrittlement in the steel. On the other hand, the oxygen reduction rate is also important during the active corrosion of steel in carbonated concrete. Since the voltages were not at corrosion potential levels in the experiments, the high cathodic currents obtained experimentally and shown in the curves were probably due to hydrogen reduction. Metal surface passivity and the concrete cover both cause an over potential in the reduction of hydrogen and oxygen. The same reasons are expected to cause small anodic currents and the experimental current values confirm this (Figs. 1-6).

Since carbon dioxide, oxygen and chloride, diffusing in the concrete, are all agents involved in the corrosion of reinforced steel, the porosity of the concrete plays a major role in corrosion. Additives or pollutants that lower the porosity of concrete or block the pores help to lower the corrosion rate by reducing diffusion. Changes in the experimental polarization curves can be explained by the change in the pore structure due to the additives LAS and LAB. Blocking of the pores and improving the metal surface coverage increases the diffusion resistance. Thus, if the effective concrete resistance ($R_c$) is increased, the oxygen diffusion rate into the concrete can be reduced substantially. The anodic branches of the current-potential curves verify the mechanisms given in previous studies[7,8,26,27], except for the current decrease due to surface cover. As seen in the reversed cathodic polarization curves, the shift in the mixed corrosion potential to the positive region proves that surface coverage thickness increases. These values show that the dissolution mechanism is similar to bare iron in similar solutions (Figs. 1-6). For the same reason, at the corrosion potential the corrosion current could not be calculated. However, at anodic potentials of the curves the effect of chloride can be seen easily. It can be seen that the anodic current values in chloride solutions are at least two times higher than those without chloride. Of course, this current is averaged over the whole steel surface and does not represent the local pitting current.

When distilled water was used as mixing water, on day 28 the compressive strength of specimens reached 31.03 MPa (Table 1); when LAS and LAB were added to the mixing water higher values were measured (in distilled water + 300 ppm LAS 47% increase, in distilled water + 300 ppm LAB 52% increase). A positive effect on compressive strength was also determined when LAS and LAB were added to 1 M NaCl environments (in 1 M NaCl + 300 ppm LAS 7% increase, in 1 M NaCl + 300 ppm LAB 22% increase). This increase in the compressive strength of concrete may be related to decreasing pore size. In the current potential curves of 1 M NaCl + 300 ppm LAS and 1 M NaCl + 300 ppm LAB environments, lower current values were observed near the mixed potential. It can be concluded that chloride ions cannot reach the metal surface (Figs. 4-6). These results may also show the porosity changes in concrete. Electrochemical data provide a useful confirmation of the porosity changes due to additives and may thus be used for investigating the optimum concrete conditions (W/C ratio, aggregate, additives, etc.)

## Conclusions

(i) The diffusion of chloride and oxygen through concrete and the reduction of oxygen on the metal surface are important parameters controlling reinforcing steel corrosion. Such diffusion may be easily measured using electrochemical polarization (Eq. 1) of an embedded steel reinforcement bar.

(ii) Potentiodynamic experiments show clearly the anodic effect of chloride ions (and the diffusion of chloride) on steel corrosion in concrete. The cathodic effect of oxygen diffusion is also seen.

(iii) The effect on the diffusion process of macromoleculer detergent additives LAS and LAB in the concrete mix can be easily seen by the electrochemical approach.

## Acknowledgment

The authors thank Prof. S.B. Lyon (UMIST, UK) for his additions to discussion and his help as a scientific anglophone.

### References

1. S. Goni and C. Andrade, **Cem. Concr. Res**., **20,** 525 (1990).
2. H.T. Cao and D. Baweja and H. Roper, **Cem. Concr. Res., 20,** 325 (1990).
3. H.T. Cao, L. Bucea and V. Sirivivatnanon, **Cem. Concr. Res., 23,** 1273 (1993).
4. J.K. Boah, S. K.Samuah and P.Le Blanc, **Corrosion, 46,** 153 (1990).
5. K. Kobayashi, K. Shuttoh ,**Cem. Concr. Res., 21,** 273 (1991).
6. M. Raupach, **Material and Struc.**, **29,** 174 (1996).
7. N.A. Darwish,F. Hilbert, W. Lorenz, H. Rosswag, **Electrochimica Acta, 18,** 421 (1973).
8. B. Yazıcı, M. Erbil, **Chimica Acta Turcica, 19,** 207 (1991).
9. R.K. Dhir, M.R. Jones and M.J. Mc Carthy, **Cem. Concr. Res., 23,** 1443 (1993).
10. A.V. Saetta, R.V. Scotta and R.V. Vitaliani, **ACI Materials Journal, 90,** 441 (1993).
11. Rasheeduzzafar, S.S. Al-Saadoun, A.S. Al-Gahtani, F.K. Dakhil, **Cem. Concr. Res**., **20,** 723 (1990).
12. Rasheeduzzafar, S.E. Hussain, S.S. Al-Saadoun, **Cem. Concr. Res., 21,** 777 (1991).
13. Reported by ACI Committee 222, **ACI** 222R-89, Corrosion of Metals in Concrete.
14. Rasheeduzzafar, S.S. Al-Saadoun and A.S. Al-Gahtani,**ACI Materials J.,89,** 337 (1992).
15. A.B. Yılmaz, B. Yazıcı and M. Erbil, **Cem. Conc. Res., 27,** 1271(1997).
16. S.H. Lin, **Corrosion, 46,** 964 (1990).
17. G. Balabanic, N. Bicanic, A. Durekovic, **Cem. Concr. Res., 26,** 761 (1996).
18. J.A. Gonzalez, C. Andrade, C. Alonso and S. Feliu, **Cem. Concr. Res., 25,** 257 (1995).
19. T. Yonezawa, V. Ashworth and R.P.M. Procter, **Corrosion**, **44,** 489 (1988).

20. J.A. Gonzalez, E. Otero,S. Feliu, **Cem. Concr. Res., 23,** 33 (1993).
21. J.T. Hinatsu, W.F. Graydon, F.R. Foulkes, **J. Appl. Electrochem., 20,** 841 (1990).
22. C. Andrade, C. Alonso, M. Acha and B. Malric, **Cem.Conc.Res., 22,** 869 (1992).
23. C. Dehghanian, C.E. Locke, **Corrosion, 38,** 494 (1982).
24. R.H. Perry and C.H. Chilton,**Chemical Engineers' Handbook,** Fifth Edition.
25. J. Avila-Mendoza, J.M. Flores and U.C. Castillo, **Corrosion, 50,** 879 (1994).
26. A.A. El Miligy, F. Hilbert and W.J. Lorenz, **J. Electrochem. Soc., 120,** 247 (1973).
27. F. Hilbert, Y. Miyoshi, G. Eichkorn and W.J. Lorenz**, J. Electrochem. Soc., 118,** (1971).